Waterborne butyl methacrylate (co)polymers prepared by Pickering emulsion polymerization: Insight of their use as coating materials for slow release-fertilizers

Asma Sofyane, Emna Ben Ayed, Mohammed Lahcini, Mehdi Khouloud, Hamid Kaddami, Bruno Ameduri, Sami Boufi, Mustapha Raihane

Waterborne Butyl Methacrylate (co)polymers Prepared by Pickering Emulsion Polymerization: Insight of their use as Coating Materials For Slow Release-Fertilizers

Asma Sofyane [a], Emna Ben Ayed[b], Mongi Elrebii[b], Mohammd Lahcini [a], Mehdi Khouloud[c], Hamid Kaddami [a], Bruno Ameduri [d], Sami Boufi[b*], Mustapha Raihane [a*]

[a] IMED-Lab. Faculty of Sciences and Techniques. Cadi-Ayyad University. Av. A. Khattabi. BP 549. 40000 Marrakech, Morocco
[b] University of Sfax- LMSE-Faculty of Science-BP 802-3018, Sfax, Tunisia
[c] UM6P-OCP-Jorf Lasfar. BP 118, 24000 El Jadida, Morocco
[d] ICGM, CNRS, University of Montpellier, ENSCM, Montpellier, France

Abstract

A new approach for preparing slow-release membranes encapsulated diammonium phosphate (DAP) fertilizer with waterborne polymers is presented. Latex dispersions based on butyl methacrylate (BMA) and 2-(perfluorohexyl)ethyl acrylate (PFA) were produced by emulsion (co)polymerization using starch nanocrystals (SNC) as a pickering stabilizer. A conversion degree exceeding 98% was reached, while the solid content was close to 20 wt %. The particle diameter distribution of PBMA homopolymer and P(BMA-*co*-PFA) copolymer dispersions as well as the contact angle measurements and thermal properties were investigated and showed that the incorporation of PFA units in PBMA improves the thermal stability and the hydrophobic character of the copolymer. The use of these (co)polymers as fertilizer coatings was explored. The morphological characterization of the coated fertilizer, performed by Scanning Electronic Microscopy (SEM), Electronic Diffraction X-ray (EDX) and mapping, revealed the formation of a cohesive film with a good adhesion between DAP fertilizer and coating films. The evaluation of the release of nutrients (N, P) in water was monitored by UV-Vis spectroscopy. Compared to uncoated DAP granules which are totally solubilized after less than 2 hours, the P release profiles of the coated fertilizers reached the equilibrium stage after 28 and 50 hours when the DAP was coated with PBMA and P(BMA-*co*-FPA), respectively. Indeed, the time to reach the maximum N release concentration was 13.5 and 16.0 times lower than the corresponding uncoated DAP when the DAP was covered with PBMA and P(BMA-*co*-FPA), respectively. These results indicated significant slower nutrients (P and N) release properties to enhance the efficiency of fertilizer use and minimize adverse environmental effects, and to match with the nutrient demand during crop growth.

Corresponding authors: M. Raihane (m.raihane@uca.ma)
S. Boufi (sami_boufi@yahoo.com)

Introduction

The United Nations projected that the global population is rapidly growing every year and should be around 9.2 billion by 2050 [1,2], hence requiring a corresponding increase in crop production and food supply. To meet the food demand of the world population and to tackle the issues of food security through sustainable agriculture, the use of agricultural inputs such as inorganic nitrogen, phosphorus and potassium (NPK) fertilizers has been reported to increase crop productivity by approximately 60%. [3] By 2050, nitrogen and phosphorus fertilizations are forecasted to increase by 2.7 and 2.4 times than the current amounts, respectively. [4] However, commonly used commercial uncoated fertilizers are water-soluble quick-release fertilizers, and are well-known for low efficiency of plant nutrients uptake caused by the high release of fertilizers rather than the absorption rate by plants, the current levels of N, P and K only reach 30-35%, 18-20%, and 35-40%, respectively. [5] These macronutrient losses on farmlands are attributed to various reasons such as runoff, leaching and volatilization. These factors not only lead to financial losses due to waste of energy related to their productions, but also induce risks for the environment such as disturbances in soil, increased concentration of greenhouse gases, and deterioration of the groundwater quality. [6,7]

A promising approach that reduces such pollution problems while also improves fertilizer utilization efficiency is the use of slow-release fertilizers (SRFs). SRFs are designed to release nutrients in a slow and delayed manner to match the nutrient demand during crop growth. [7] Therefore, the SRFs products show a great potential in improving fertilizer use efficiency and alleviating environmental issues induced by fertilizer management. [8] Generally, SRFs products prepared by encapsulating fertilizer granules with hydrophobic polymer materials are one of the most widely used types of SRFs that serve as a diffusion barrier. Besides fertilizer, water is another important factor that plays an essential role in agriculture. [9] In this context, the development of SRFs with high water-retention capacities is of great interest for modern agriculture. Several polymer materials have been proposed for SRFs encapsulation. They are mainly divided into two categories according to the solvent types used in SRFs production. Polymers such as polyolefins are usually soluble in organic solvents to obtain polymer solutions used to encapsulate the surface of fertilizers. [10] This coating process requires costly volatile organic solvents and may lead to a secondary pollution. [11] Indeed, more and more attention is paid to waterborne coatings, which have the advantage of nontoxicity, nonflammability, low price, and good quality in comparison with the traditional organic coatings. [12] In fact, especially in arid and semiarid regions, many farmlands suffer from water resource shortages and thus it is essential to use water resources efficiently. Hence, application of superabsorbent polymers

(SAPs) in agriculture has got encouraging results, namely, improved water-holding capacity, reduced irrigation frequency, and lower death rate of plants because of excellent water absorption capacity and water-retention properties of SAPs. [13] Among these SAPs, poly(acrylates) (PAs) have been used in the field of agriculture as coatings for SRFs. [14,15] PA coated SRFs increase wheat and maize crop yields in the North China Plain [16] and India. [17] PAs adopt waterborne coating technology by using aqueous solution in production. These polymer materials have good film-forming properties and are relatively cheap. [13] Furthermore, PAs were obtained by aqueous free radical (co)polymerization of acrylic monomers such as acrylic acid (AA), acrylamide (AA_m), methacrylic acid (MA) initiated by ammonium persulfate and in the presence of N,N'-methylenebisacrylate (MBA) as a cross-linking agent to obtain networks with improved water-retention capacity and slow release nutrients. [15, 18] To improve the soil water retention, increasing attention has been focused on superabsorbent hydrogels, which are able to absorb and preserve large amounts of aqueous solutions. [19] Among various superabsorbent hydrogels, semi-interpenetrating polymer networks (Semi-IPN) are gaining increasing attention as SFR, for which hydrophobic polymers such as poly(vinyl alcohol) (PVA) or poly(vinylpyrrolidone) (PVP) were mixed to the cross-linked PA to make non-covalent interactions. [9,15, 20] Indeed, PAs are reported to be biodegradable in the soil at rates of 0.12–0.24% per six months. [21] Thus, the development of eco-friendly natural-based super swelling hydrogels has drawn much interest owing to their abundant resources, low production cost and biodegradability. Hydrogels based on totally/partially renewable polymers are classified into polysaccharide and carbonaceous-based kinds where "grafting on" radical polymerization of acrylic monomers occurred. Indeed, nanofillers such as clays (*e.g.* montmorillonite (MMT) and bentonite (Bent)) have been also added to these PAs latexes to improve their mechanical properties, to increase holding water and reduce the price. Wen et al. [9] reported the preparation a Semi-IPN cotton stalks-*g*-poly(AA)/PVP/Bent for slow nitrogen fertilizer, 60% of nutriment were released after 30 days, while Olad et al. proposed a strategy based on the incorporation of MMT into semi-IPN sodium alginates (NaAlg)-*g*-poly(AA)/PVP hydrogel. [22] Superabsorbent composites based on chitosan-*g*-poly(AA_m)/MMT were synthesized through *in-situ* grafting radical polymerization in presence of MMT at different contents. The introduced montmorillonite could form a loose and porous surface and improve water absorption of the superabsorbent. [23] These SAPs were prepared by aqueous radical free polymerization without any surfactants.

In contrast to the PAs, polymers based on fluorinated acrylates exhibit remarkable properties such as thermal stability, chemical inertness, and low surface tension. [24] Several acrylate and

methacrylate polymers bearing perfluoroalkyl side chains (*i.e.* C_6F_{13} and C_8F_{17}) show good hydrophobicity comparable to the corresponding n-alkyl chains because the side chains are more rigid than n-alkyl chains thus enhancing the water repellent properties. [24,25] Therefore, homopolymers and copolymers based on fluorinated (meth)acrylates have been used as coatings. [26-28] Chen et al. [29] reported the synthesis of a novel slow-release coated urea by coating fertilizer with water-based hydrophobic polymers obtained both 1H,1H,2H,2H-perfluorooctyltriethoxysilane and nano-SiO_2 to modify the water-based polymer.

Emulsion polymerization provides a sustainable way to produce latex polymers for coatings and adhesives thanks to the use of water as a dispersion medium. In fact, waterborne acrylic, obtained by radical emulsion polymerization of n-butyl acrylate (BA), methyl methacrylate (MMA) and methacrylic acid (MA), and modified with organic siloxanes were synthesized to increase the nutrient release duration. [29] Composites based on modified PAs with graphene oxide (GO) were applied as coatings for controlled-release coated urea, and thus dramatically slowing down the cumulative nutrient release from the SRF from 87.25% to 59.71%. [30] These waterborne PAs were prepared by aqueous radical free polymerization using commercial synthetic surfactants (*i.e.* Sodium dodecylbenzene sulfonate, nonyl-phenyl-polyroxyethylene ether-10), which are harmful to environment. This synthesis approach can be even more attractive if synthetic surfactant can be replaced by biobased solid particles as a stabilizer, through the ‘‘Pickering effect”. Pickering emulsion polymerization consists in the use of solid particle as stabilizer to impart colloidal stability during the generation and growth of polymer particle throughout the polymerization reaction. Recently, the use of biobased nanoparticules as Pickering stabilizer have aroused much interest for the evident advantages incoming for their presence, including biodegradability, safety to use, environmentally friendly, and biocompataibility. Cellulose nanocrystals (CNC) [31] and starch nanocrystals (SNC) [32] have been successfully used as stabilizers in Pickering emulsion polymerization of numerous acrylic and vinylic monomers along with the possibility to produce polymer latex with solid content exceeding 30%, which is prerequisite if any industrial application is considered.

The objectives of this present work aim at investigating the use of SNC as Pickering stabilizer by varying its amount in emulsion (co)polymerization of butyl methacrylate (BMA) with a fluorinated comonomer namely 2-(perfluorohexyl)ethyl acrylate (PFA) without adding any surfactant or costabilizer. To the best of our knowledge, the synthesis of such fluorinated acrylate copolymer using SNC as a pickering stabilizer has not been reported in the literature yet. Both PBMA and P(BMA-*co*-PFA) waterborne acrylic emulsions, prepared using 8 wt% of SNC in fertilizer coating, was performed. The morphology and the chemical composition of

the surface and cross-section of coated fertilizers were investigated by SEM-EDX, while the release profiles of their nutrients (N and P) were carried out using UV-visible spectroscopy. The structure (introduction of fluorinated acrylate)-release behavior relationship has been studied to evaluate the performance in terms of increasing the release nutrients duration of these new latexes acrylic coatings.

2. Experimental section

2.1. Materials

Butyl methacrylate (BMA, 99 wt%) was purchased from Sigma-Aldrich, while 2-(perfluorohexyl)ethyl acrylate (PFA) was kindly supplied by Atofina (Pierre Bénite, France). These monomers were distilled, and then stored in a fridge at 5 °C prior to use. Hydrogen peroxide (H_2O_2), citric acid (CA), and sulfuric acid were purchased from Aldrich and used without further purification. Waxy maize was kindly provided by Roquette S.A. (Lestrem, France) while diammonium phosphate (DAP), a granular phosphate fertilizer (46% P_2O_5), is a gift from OCP Group (El Jadida- Morocco). Distilled water was used for all the polymerization and treatment processes.

2.2. Starch nanocrystal preparation

Starch nanocrystals (SNC) were prepared by sulfuric acid hydrolysis of waxy maize starch as described in details in previous works. [33,34] Briefly, 5 g of starch were added to 3.16 M aqueous sulfuric acid solution and left under stirring at 40 °C in a thermostated bath for 5 days. Then, the suspension was centrifuged at 10,000 rpm to recover the SNC. The SNC nanoparticles were centrifuged repeatedly with distilled water until neutrality. A homogeneous dispersion of starch nanocrystals was obtained by using a T25UltraTurrax homogenizer for 3 min at 13500 rpm at room temperature.

2.3. Emulsion (co)polymerization

The emulsion copolymerization of BMA and PFA in the presence of different weight ratios of SNC was carried out as follows: calculated weight percentages of SNC (4-10 wt% based on the amount of monomers) were first dispersed in water by gentle sonication for 1 min at a 70% amplitude (Sonics Vibracel Model CV33) to ensure the effective disintegration and individualization of SNC in water. Then, the mixture of monomers and citric acid was added and emulsified by vortexing for 2 min. After flushing with N_2, the kit was placed in a heated

bath at 50 °C and the polymerization was run by adding 0.15 g of H_2O_2 for 1.5 h. The polymerization was continued for additional 3 h. In all cases, a conversion degree exceeding 98% was reached within a 4.5 h of polymerization, while the solid content percentage was close to 20 wt %. Once the polymerization was achieved, 0.10 g of 0.1% of NaN_3 aqueous solution was added to prevent from bacterial growth. The resulting copolymers were referred to as P(BMA-*co*-PFA) X%, where the feed molar percentages of BMA and PFA were 90 and 10, respectively, while X corresponds to the content of SNC during the copolymerization.

The poly(butyl methacrylate) homopolymer, PBMA, was also synthesized to be used as a reference material according to the same experimental protocol. The synthesis route is displayed in Scheme 1 and the typical formulations for the emulsion homo and copolymerization of BMA in the presence of SNC are supplied in Table 1.

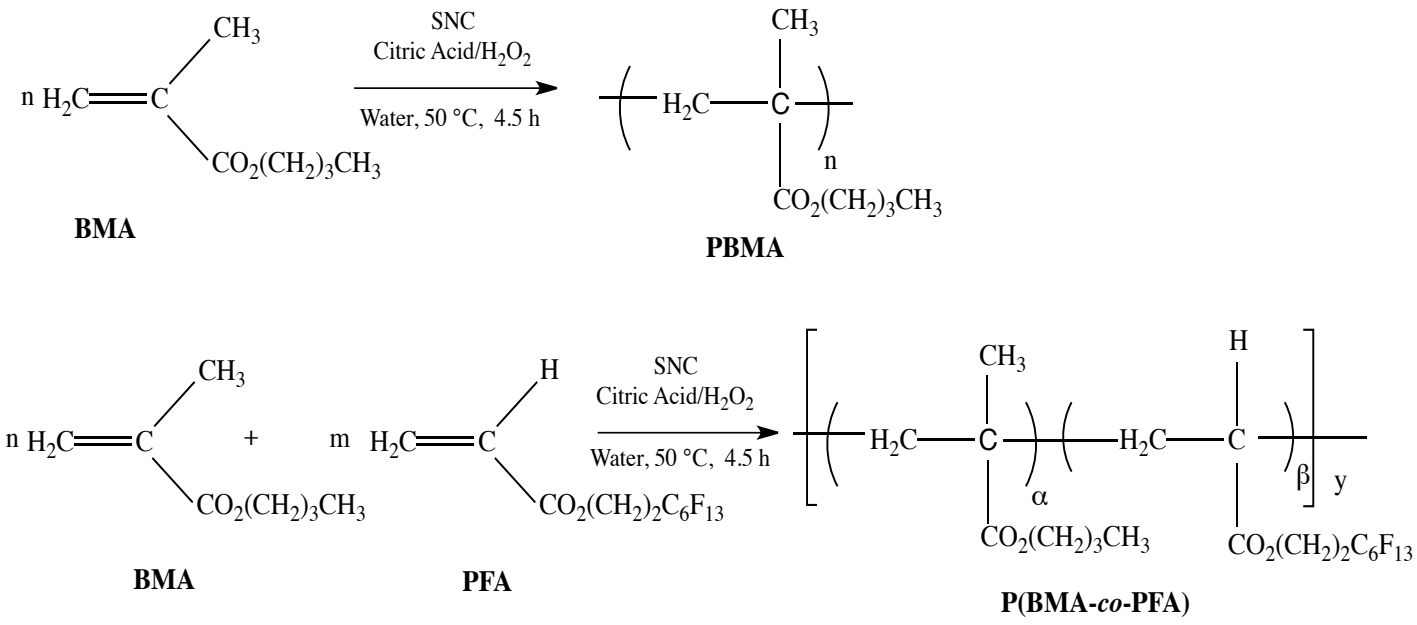

Scheme 1: **Radical emulsion homopolymerization of BMA, and copolymerisation of BMA with PFA initiated by H_2O_2/Citric acid in deionized water (**$[BMA]_0/[PFA]_0$= 90/10 in the feed) **(SNC stands for starch nanocrystal as pickering stabilizer emulsion).**

Table 1. Emulsion homopolymerization of BMA and copolymerization of BMA with PFA in presence of SNC as the sole stabilizer, carried out at 50 °C (t=4.5 h, R% =98%)

Constituent	Composition (g)	
	PBMA	P(BMA-*co*-PFA)
Water	20.00	20.00
BMA	4.00	3.60
PFA	0.00	0.40
H_2O_2	0.15	0.15
CA[1]	0.15	0.15
SNC	0.32	0.16-0.30[2]

[1] *CA : Citric Acid.*
[2]. *wt % of SNC: 4-10 % based on the amount of monomers.*

2.3. Preparation of coating DAP Fertilizers

The commercial granular DAP fertilizers produced by OCP group were sieved to select with homogeneous granules with diameters of 2-4 mm and similar weight (ranging between 34.00 to 34.90 mg) before used in the laboratory test to prepare coated granules.

The coating was performed following the dip-coating process [36,37], where the DAP fertilizer was successively immersed in the emulsion solution of both PBMA homopolymer and P(BMA-*co*-PFA) copolymer prepared in the presence of 8 wt. % of SNC. The DAP pellets were then removed from solution and placed on a Teflon ® film surface. They were dried at room temperature for 1 hour. Figure 1A represents a visual aspect of the coated DAP fertilizer granules compared to uncoated DAP, which indicates that DAP granules were covered by the film coating.

Figure 1. (A): Images of: uncoated DAP (a), DAP coated with PBMA 8% SNC (b) and DAP coated with P(BMA-*co*-PFA) 8 wt % SNC (c). (B): Visual aspect of: PBMA (d) and P(BMA-*co*-PFA) (e) dispersions after emulsion (co)polymerization in the presence of 8 wt % SNC.

2.4. Polymer particle size

The diameter of the polymer particles in the emulsion was measured at 25 °C using a Malvern Nano ZS Zetasizer instrument at a fixed scattering angle of 173°. The dispersion was diluted to about 5 wt% with distilled water before starting the measurements. The particle size was expressed as a Z-average corresponding to the diameter of an equivalent hard sphere having the same diffusion coefficient as that of the particle being measured. Each measurement was performed in triplicate and the values were averaged to obtain the mean particle diameter.

2.5. ζ-Potential measurement

The ζ-potential was measured at 25 °C using a laser Doppler electrophoresis apparatus (Malvern Nano-Zetasizer ZS, UK). The sample consistency in water was set to 0.01% (w/v). The measurements were repeated three times for each sample.

2.6. Field-emission scanning electron microscopy (FE-SEM)

Small amounts of freeze-dried latex powder were deposited on silicon wafers and coated with a 2–3 nm-thick carbon layer by ion sputtering. Images were recorded using an in-lens secondary electron detector in ZEISS Ultra 55 and Gemini SEM 500 microscopes equipped with field-emission (FE) guns and operated at a 2-5 kV acceleration voltage.

For analysis of the surface and the cross section of the coated fertilizers, the granules were cut in half with a razor blade and fixed on a support. The samples were dispersed on a carbon ribbon attached to the surface of a metal disc with double-sided adhesive tape. Indeed, elemental mapping showing the spatial distribution of elements in the analyzed surface was also examined by FE-SEM. For thickness measurements of coating layers, the drawing rule option of SEM was used, and the measurements of different areas on each granule were performed. `

2.7. Thermogravimetric analysis (TGA)

TGA was carried out under air flow using a thermogravimetric analyzer (TGA 400 Perkin Elmer), with a heating cycle from 40 °C to 700 °C at a rate of 10 °C /min.

2.8. Differential scanning calorimetry (DSC)

DSC measurements were performed using a Perkin-Elmer Pyris Diamond DSC under nitrogen flow from -50 °C to 150 °C, with a heating rate of 10 °C.min^{-1}. The T_g adopted corresponds to the inflection point in the heat-capacity jump.

2.9. Water contact angle measurements (WCAs)

WCAs were carried out at room temperature using a OCA Neurtek contact angle instrument. The system was equipped with a video camera and image analyzer. Measurements were performed in triplicate by deposition of 5 μL deionized water droplets on the surface of each sample at different spots using a micro-syringe. An average of three measurements was supplied.

2.10. Release Essays of Nitrogen and Phosphorus in Water

Uncoated and coated DAP granules (100 mg) were immersed in 250 ml beakers of distilled water by continuous and slight stirring at 25 °C. Three samples of 1 µl were collected at different time intervals, diluted 100 times and analyzed in the spectrophotometer. The release profiles of nitrogen (N) and phosphorus (P) in distilled water were determined by colorimetric methods, using Indophenol reagent and Ammonium-molybdate/ascorbic acid methods (AFNOR-T90-015) and (AFNOR-T90-023), respectively. [38] The forming blue complexes were analyzed at wavelength of 880 and 630 nm for P and N, respectively, using ultraviolet–visible spectrophotometer (UV-2600, Shimadzu).

2.11. Mathematical modeling

To gain insight in understanding the nutrients release characteristics of the coated DAP, the semi-empirical Ritger-Peppas model was used to calculate the kinetic parameters according to equation 1 [39]:

$$\frac{M_t}{M_\infty} = k\, t^n \qquad \text{Eq.1}$$

where M_t and M_∞ represent the amounts of nutriment released at t and equilibrium times, respectively, k is the diffusion constant, which depends on the type of coating material, while n is a diffusional exponent characterizing the release mechanism. [40]

Diffusion coefficient (*D*) was calculated from Equation 2:

$$\frac{M_t}{M_\infty} = 4\left(\frac{Dt}{\pi l^2}\right)^{0.5} \qquad \text{Eq.2}$$

where *l* is the thickness of the composite film.

3. Results and discussion

3.1 Preparation of polymer latexes

Butyl methacrylate (BMA) was chosen as the monomer because of its low water solubility (32 mmol L^{-1} at 70 °C [41]) and high propagation rate constant (1243 dm^3 $mol^{-1}s^{-1}$ at 70 °C [42]). The evolution of the main colloidal parameters in the seeded starved-feed semi-continuous emulsion polymerization of BMA was investigated using two surfactants, the anionic SDS and the nonionic Brij 58P. [43] In order to obtain a low level of surface energy, the surface of fluorinated acrylic (co)polymer should be covered by as many fluorine-containing groups as possible. That is why 2-(perfluorohexyl)ethyl acrylate (PFA) has been chosen as a comonomer of BMA. Indeed, the cost is also reduced because less fluorine-containing monomer (PFA) was used. Therefore, the emulsion polymerization was carried out from an initial BMA/PFA molar ratio equal to 90/10. The resulting copolymer was referred to as P(BMA-*co*-PFA).

The reactivity ratios were used to deduce the behavior of both comonomers in the copolymerization reaction. The expected monomer reactivity ratios, $r_1=r_{BMA}$ and $r_2=r_{PFA}$ of BMA and PFA, respectively, may be calculated from their empirical Alfrey-Price *Q* and *e* parameters [44] as described in the Electronic Supporting Information (ESI). Equations S2 and S3 lead to the following values: $r_1=r_{BMA}$ =1.42 and $r_2=r_{FPA}$ 0.70 at 50 °C. The reactivity ratio of BMA was higher than that of FPA, which indicates that the copolymer contains more BMA than PFA comonomer compared to those in the feed. Indeed, r_1 >1 and r_2 <1 implies that the rate constants *k* can be compared as follows: $k_{11}>k_{12}$; $k_{22}<k_{21}$ showing that one of both comonomers (BMA) is more reactive than the other one toward both macroradicals. In addition, r_1 x r_2 product worths 0.99 that is close to unity, indicating that there is a random distribution of both comonomers along the copolymer chain, thus explaining its statistical structure.

The molar composition of both comonomers in P(BMA-*co*-PFA) copolymer can be assessed using the composition equation S4. As the molar ratio of BMA (f_1) and PFA (f_2) in the feed is 0.9/0.1, the calculated molar percentage of incorporated BMA in P(BMA-*co*-PFA) copolymer (F_1) was close to 93% (F_2=7% of PFA). It means that BMA incorporates faster than the PFA monomer does into the growing copolymer chain which is in good agreement with the reactivity ratio ($r_1=r_{BMA}$>1). The molar incorporation ratio of PFA monomer in purified P(BMA-*co*-PFA) copolymer, assessed by elemental analysis (%O= 20%) according to equation S5, is close to 6.5%, and matches that calculated from the reactivity ratio.

In the emulsion polymerization, the residual synthetic emulsifier in latexes would have adverse effects on the properties of the products and can even induce some environmental pollution. In

order to avoid the disadvantages resulting from emulsifier, biobased modified SNC as pickering emulsion surfactant is used in this study. Compared to the surfactant-stabilized emulsions where the stabilization is driven by the reduction in the interfacial tension, in pickering emulsion, the stabilization is due to the reduction of the bare oil-water interface through the adsorption of solid particles, which creates a physical barrier against the coalescence of the dispersed phase and blocks the Ostwald ripening process. [44, 45]

SNC were produced following the well-known sulfuric acid hydrolysis route during several days. Figure 2 displays the particle diameter distribution, the ζ-potential, and the TEM images of SNC.

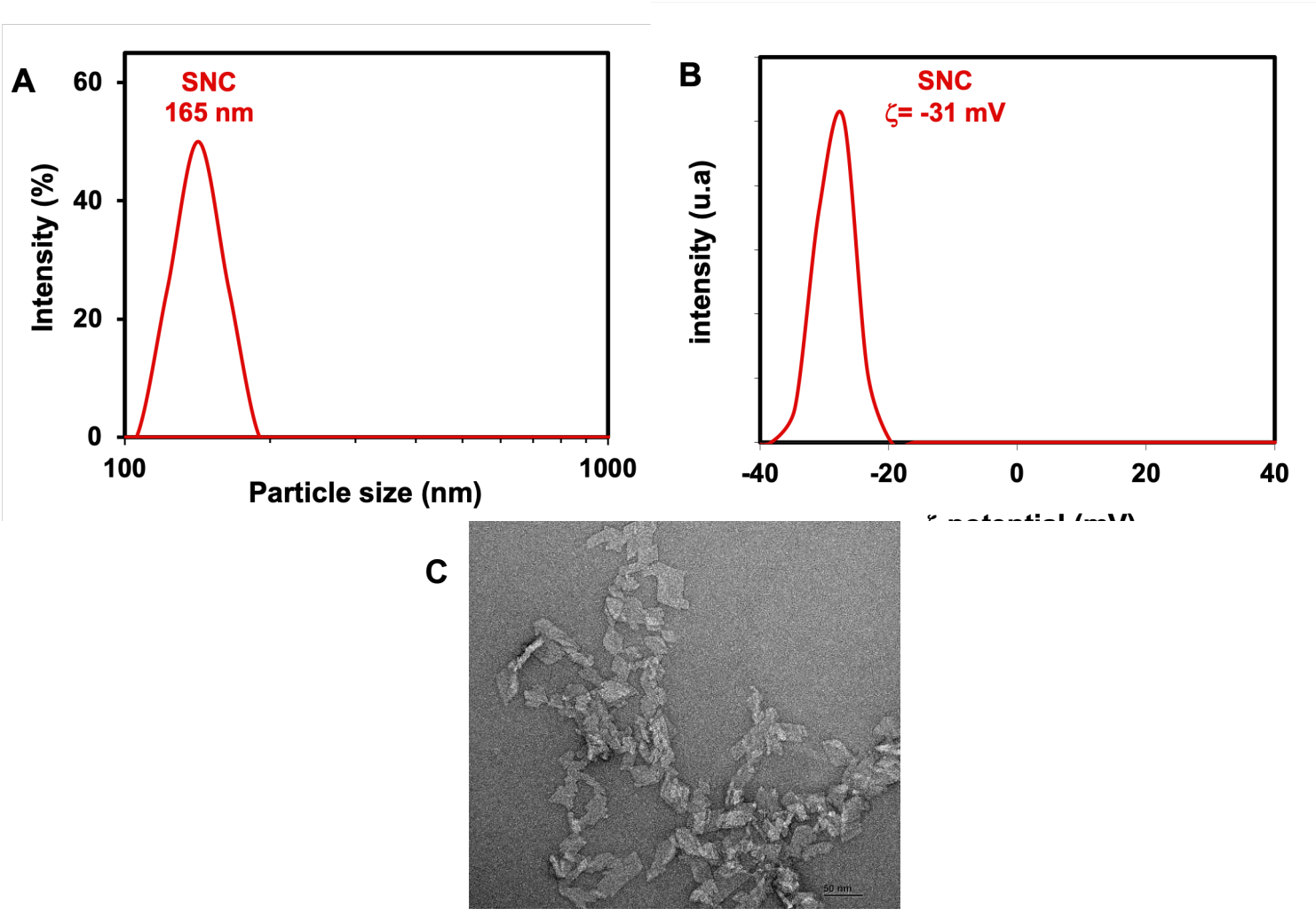

Figure 2. (A) Particle diameter distribution, (B) ζ-potential, and (C) TEM images of SNC (bare scale : 50 nm).

The dynamic light scattering (DLS) measurement on a sonicated diluted suspension of SNCs (Figure 2A) gave a monomodal size distribution centered at around 165 nm with a polydispersity index (PDI) close to 0.11 indicating a narrow size distribution. The ζ-potential

of the particles (Figure 2B) was around -31 mV and remained negative over the whole pH range from 2 to 12, which results from the presence of the sulfate groups ($-OSO_3^-$) at the surface of SNC resulting from the esterification reaction during sulfuric acid hydrolysis. [44] TEM observation (Figure 2C) revealed a platelet like shape with a polygonal form and a size ranging between 40 and 140 nm.

The emulsion polymerization was performed in batch by mixing the monomers with SNC suspension without any surfactant and progressive addition of the initiator over 1.5 h at 50 °C. The selection of this relatively low polymerization temperature was considered to avoid any risk of dissolution of starch crystallites. This low temperature also justifies the necessity to use citric acid as catalyst to accelerate the decomposition of H_2O_2 via a redox process [46] and provides enough hydroxyl radical during the whole emulsion polymerization. During the first hour, the monomer remained in the form of a coarse visible droplet and the medium turned hazy and then milky, giving rise a milky fluid dispersion without any significant evolution in viscosity at the end of the polymerization. However, the colloidal stability of the latex dispersion was dependent on the used SNC amount. A stable coagulum-free latex dispersion was obtained only if the SNC is higher than 4 wt. %, and as long as the amount of SNC exceeded 6 wt.%, the latex dispersion was stable for several months at room temperature, without any sign of decantation or aggregation of polymer particles. Figure 1B displays the visual aspect of PBMA and P(BMA-*co*-PFA) dispersions after emulsion (co)polymerization in the presence of 8 wt. % SNC.

Figure 3 displays the particle size distribution of (co)polymers latex dispersions at different SNC contents, and the corresponding contact angles of the obtained films, while Table 2 summarizes the obtained data of P(BMA-*co*-FPA) copolymers *versus* the SCN amounts.

Table 2. Particle size distribution and water contact angle measurements (WCA) of P(BMA-*co*-FPA) copolymer latex dispersions prepared by emulsion copolymerization at different SNC contents at 50 °C (t=4.5 h, conversion =98%, solid content = 20%)

wt.% SNC	Particule size (nm)	WCA (°)
4	342	73
6	255	75
8	220	80
10	190	89

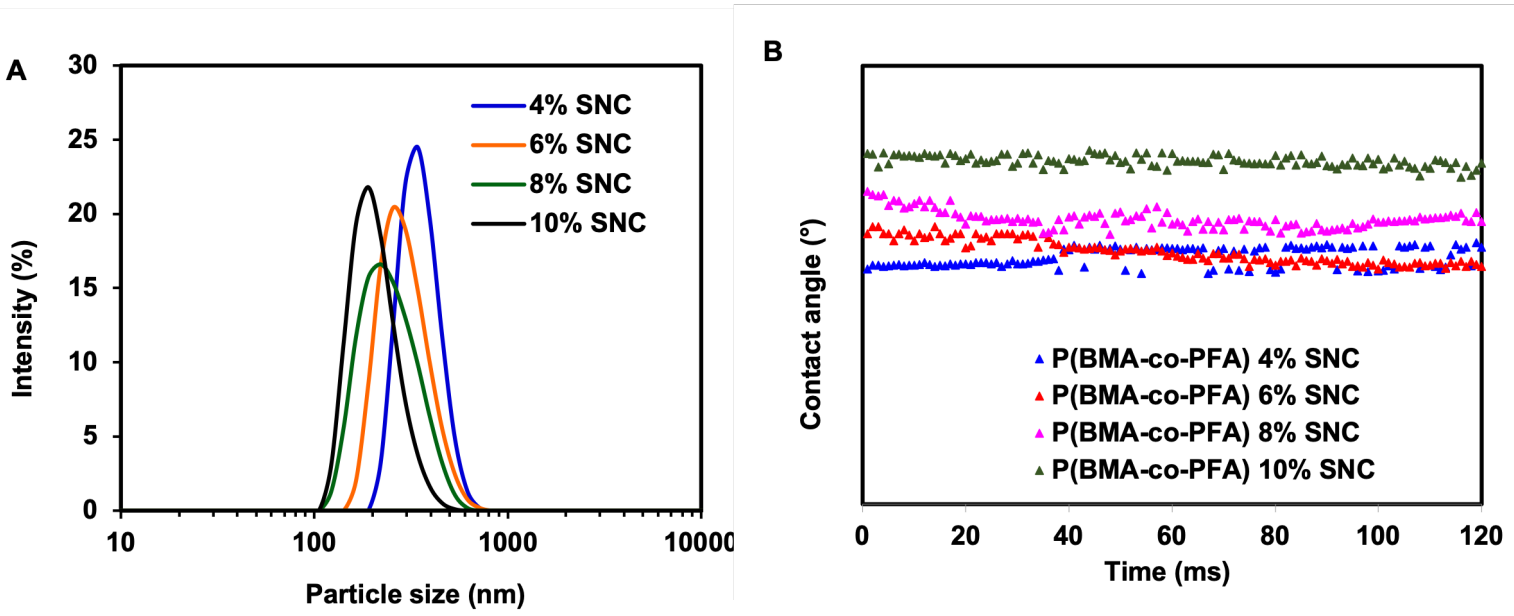

Figure 3. (A) Particle size distribution of P(BMA-*co*-PFA) latex dispersions prepared via pickering emulsion polymerisation at different SNC weight per, and (B) water contact angles *versus* times of the film from the latex dispersion.

Figure 3A shows a monomodal distribution in particle size for all P(BMA-*co*-PFA) copolymer latexes with mean particle size ranging from 200 to 500 nm, depending on the SNC content. A clear tendency to a decrease in the particle size is observed as the added SNC amount is going up.

At 4 wt. % SNC, the particle size of the polymer dispersion was around 350 nm and decreased to about 190 nm when the polymerization was operated in presence of 10% SNC. This close dependence of the particle size on the amount of added SNC demonstrates the key role of SNC in the stabilization process and evidences the strong SNC efficiency as a pickering stabilizer in emulsion polymerization of acrylic monomers. [35] This result is in agreement with our previous work and confirms that the stabilization aptitude of SNC is operative also in emulsion copolymerization, where two comonomers of different structure and hydrophobicity have been involved. [47] Similar results were reported for PBMA where the particle size of the latex dispersion reached about 600 nm for 4 wt.% SCN content and decreased to *ca.* 280 nm when the SNC amount increased to 10 wt.% [44]

The effect of PFA addition on the hydrophobic property of the film obtained by casting the latex solutions onto a glass substitute was assessed by measuring the water contact angle (Figure 3B). Result indicated that the contact angle of the P(BMA-*co*-PFA) copolymer film containing 6.5 wt. % of PFA in the copolymer changes according to the content SNC in

the dispersion. The water contact angle for PBMA film was around 74° and those of P(BMA-*co*-PFA) reached the values of 73°, 75°, 80° and 89° for SNC content of 4, 6, 8 and 10 wt. %, respectively. This means that the hydrophobic character of the film increased with the SNC content during the emulsion polymerization. One possible reason accounting for this unusual behavior would be the preferential accumulation of the fluorinated monomer at SNC surface which leads to a generation of a gradient composition in the structure of the copolymer. In fact, for polymeric materials, the surface energy value is determined mainly by the chemical structure at the surface: it has been established that the surface energy of the constituent groups decreases by the following order: CH_2 (36 mN m^{-1})> CH_3 (30 mN m^{-1})> CF_2 (23 mN m^{-1})> CF_3 (15 mN m^{-1}). [48] Therefore, the fluorinated polymers such as P(BMA-*co*-PFA) possessing the flexible linear zig-zag-shaped skeletons in the side chain exhibits lower surface energy values and therefore an improvement of its hydrophobic character compared to that of the non-fluorinated polymers such as PBMA. [24,25]

The morphology of the polymer dispersion observed by FE-SEM (Figure 4) revealed polymer particles with spherical shape and size ranging from 100 nm to about 1 µm, which is in agreement with DLS measurements. From FE-SEM observation, it was not possible to distinguish the SNC on the surface of polymer particles.

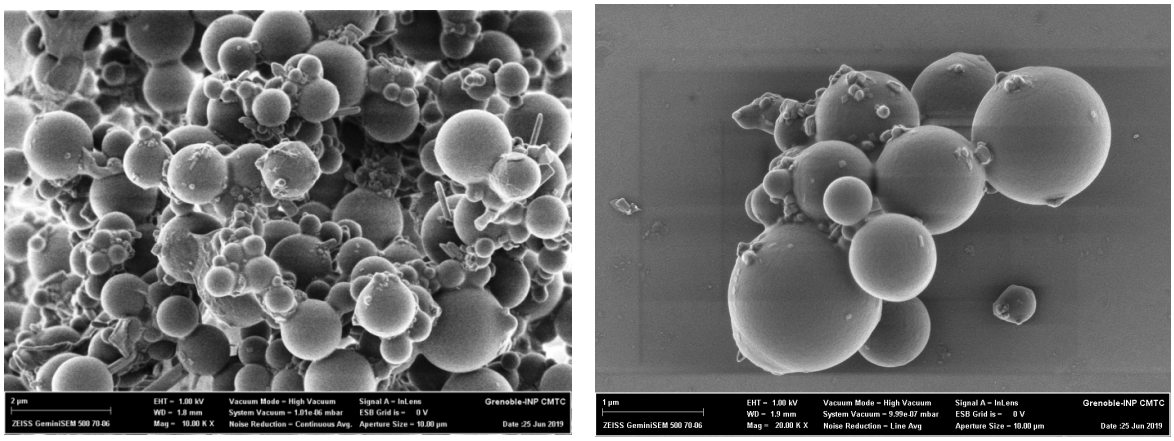

Figure 4. FE-SEM images of freeze-dried P(BMA-*co*-PFA) latex dispersion, at different magnification, prepared in the presence of 8 wt% SNC.

The thermal properties of the PBMA and P(BMA-*co*-PFA) copolymer were studied by DSC and TGA (Figure 5).

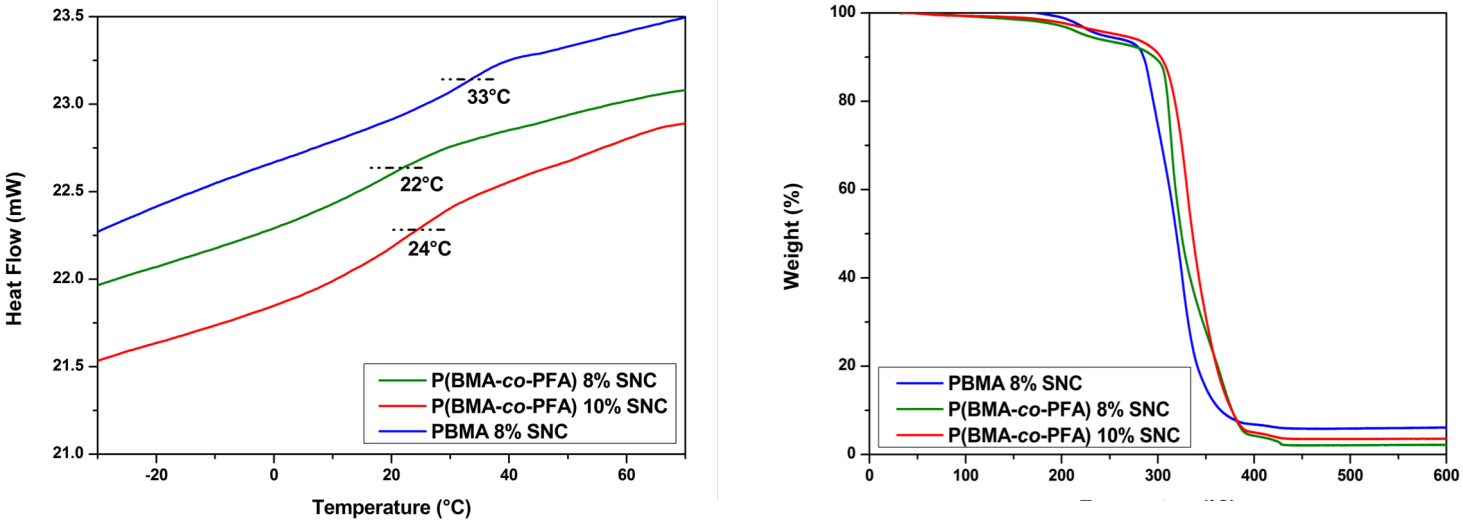

Figure 5. DSC and TGA thermograms of PBMA and P(BMA-*co*-PFA) (at two SNC contents) films from latexes produced by emulsion (co)polymerization in presence of SNC as stabilizer.

The glass transition temperatures (T_gs) of PBMA and P(BMA-*co*-PFA) prepared in presence of 8 wt. % SNC were *ca.* 33 and 24 °C, respectively (Figure 5). Moreover, no melting point was observed which confirms the amorphous structure of these (co)polymers. In contrast, the polyacrylates with perfluorooctyl (-C_8F_{17}) side chains lead to hexatic smectic phases which are responsible of the presence of isotropization temperature PFA-C_8F_{17} (79 °C). [25]

Compared to PBMA homopolymer, the decrease in the Tg in the copolymer film is expected, considering the long chain of the acrylate moiety (8 methyl groups: $CO_2CH_2CH_2C_6F_{13}$) imparting an internal plasticizing effect. The decrease in the Tg is beneficial for film-formation to occur spontaneously at room temperature as long as the temperature remained around 20 °C. At higher SNC content (10 wt. %) used in the emulsion polymerization did not affect the Tg value, which is presumably due to the localization of SNC around the polymer particles.

The TGA thermograms of PBMA and P(BMA-*co*-PFA) under air flow are shown in Figure 5. The PBMA prepared by emulsion polymerization in presence of SNC was stable up to 220 °C and showed a mild loss of about 4-6%, presumably associated to SNC thermal degradation. [49] Then, an abrupt weight loss of more than 90% was observed between 280 to 340 °C, is attributed to the thermal cleavage of alkyl groups from the side chain and followed by some depolymerization reaction. ~~The decomposition of polyacrylates and of both kinds of polymers with long fluoroalkyl side chains also yielded fluorinated alcohols, dimer, saturated diester, trimer, etc~~. [26, 50, 51] Indeed, the inclusion of fluoromonomer seems to delay the thermal

degradation of the methacrylate backbone by about 20 °C, which is likely due to the better thermal stability of the C_6F_{13} pendant group in PFA moiety attributed to the strong C-F bonds (485 kJ/mol). [21]

3.2 Water release essays of coated DAP

This study is focused on investigation of release behavior of P(BMA-*co*-PFA) 8 wt. % SNC and compared with that of P(BMA) homopolymer as a reference, to highlight the changes introduced by the incorporation of the hydrophobic PFA comonomer on the kinetic release of nutrients (N and P).

3-2-1 Morphological characterization of coated DAP fertilizers

The surface and cross-section of uncoated DAP and coated DAP morphologies were examined by FE-SEM, and their micrographs are shown in Figure 6.

Fig. 6a displays the surface of uncoated DAP granule which presented a rough and uneven structure containing small pores observed at high magnitude on its surface (Fig 6b-c). When the DAP fertilizers were encapsulated by both polymers based on BMA, the coating surfaces show a smoother and denser structure that the uncoated DAP (Figs 6d, e, g and h). [38] Similar observations were reported by Dubey et al. [52] by comparing the surface morphology of urea before and after coating by zeolite and acrylic polymer blends.

Fig. 6f and Fig. 6i show the cross-section micrographs SEM of coating materials with different magnitudes. The inter-juncture zone of both coated materials (PBMA and P(BMA-*co*-FPA) 8% wt. SNC) and DAP fertilizers is continuous and devoid of any gap or cavity present in between them. The formation of cohesive films with different thicknesses are observed and confirmed that polyacrylates (PAs) have a potential to be used in the field of agriculture as coatings for slow-release fertilizers. [14,15] Indeed, the border and adhesion between DAP and the film coating is irregular and sometimes difficult to observe, most likely due to the non-spherical shape and irregular surface of the initial DAP granules. [53] The thickness was taken at three different locations and the average thickness is calculated (Figures 6f and 6i). The coating thicknesses average are approximately closed to 39±5 and 34±5 µm when the DAP fertilizers were coated with P(BMA-*co*-PFA) and PBMA, respectively (Fig. S1 in ESI).

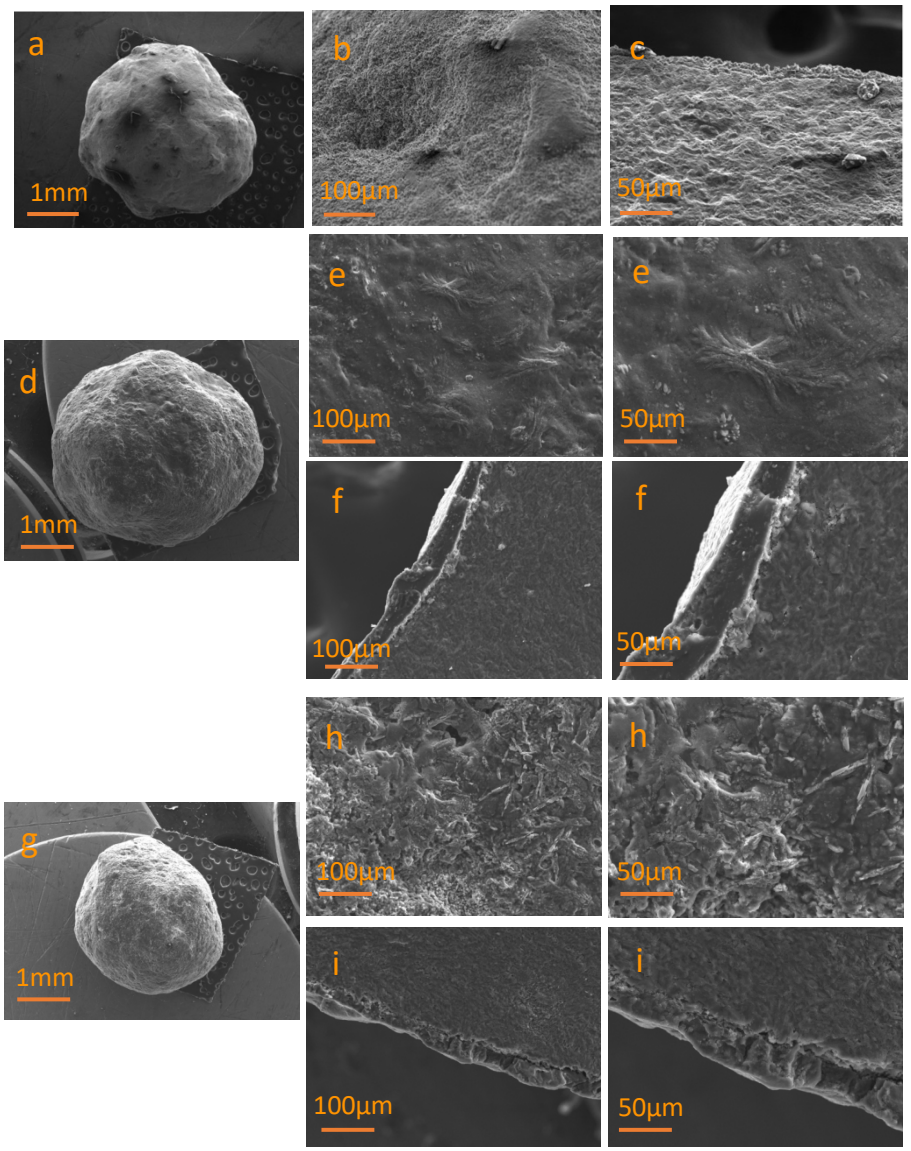

Figure 6. SEM images of uncoated DAP (a: granule, b: surface and c: cross- section), DAP coated with P(BMA-*co*-PFA) 8% wt. SNC (d: granule, e: surface and f: cross-section) and DAP coated with PBMA 8% SNC (g: granule, h: surface and i: cross-section).

The comparison of the EDX signals before and after coating (Fig. S2 in ESI) revealed definite changes between the surfaces of coated and uncoated granules. The EDXs results are summarized in Table 1. Indeed, the spectra of uncoated granules display characteristic peaks of phosphorus (P) and nitrogen (N), which are assigned to the nutrients of DAP fertilizer. The percentage of macronutrient elements such as P (21.5%) is close to those reported by the OCP Company (P 20.1% (or 46% as P_2O_5)), [54] and other micronutrient elements with low percentage such as Mg were also noted. The detected carbon (19.5 %) corresponds to that used during the metallization of the DAP granule in order to make the analyzed sample surface conductive and to detect it later in the SEM analyses.

Indeed, EDX analyses can generate information about the chemical composition of uncoated and coated fertilizers (Table 3). For the DAP coated with both polymers, the carbon percentage increases compared to that of the uncoated fertilizer and is attributed to carbon of the incorporated (meth)acrylic monomers units. Indeed, the oxygen % is higher when the fertilizers are encapsulated with P(BMA-*co*-PFA) than those coated with PBMA, as excepted since the copolymer contains two ester groups in contrast to only one for PBMA homopolymer. Moreover, the presence of fluorine atoms in the copolymer (%F: 1.3 %) confirms the presence of PFA units in the fluorinated coatings prepared from 10% feed PFA comonomer. Compared to uncoated DAP, the P % decreases when the fertilizers were recovered by the (co)polymer.

Table 3. EDX analyses of uncoated DAP and coated DAP with PBMA and P(BMA-*co*-PFA) copolymer.

		Elemental weight percentage (wt. %)							
		C	P	N	O	F	Mg	Si	S
Uncoated DAP		19.5	21.5	10.1	46.9	0.0	0.4	0.0	0.0
DAP coated	P(BMA-*co*-FPA)	71.4	3.7	0.0	20.0	1.3	1.3	2.3	0.0
	PBMA	81.4	1.3	0.0	14.8	0.0	0.0	1.8	0.8

Figure 7 displays the EDX mapping and shows the distribution of the elements (C, P, N and O) on the cross-section of DAP coated with both PBMA and P(BMA-*co*-PFA).

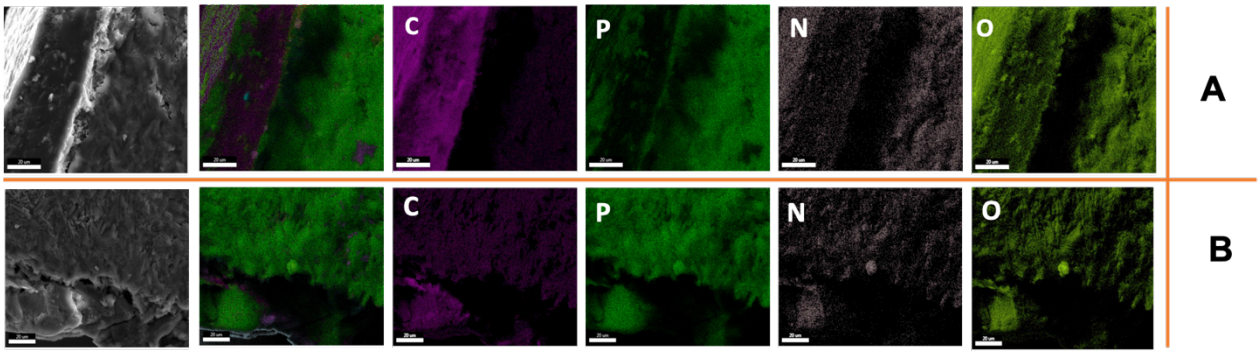

Figure 7. Spatial distribution of the elements (C, P, N and O) on the cross sections of: (A) DAP coated P(BMA-*co*-PFA) 8%SNC and (B) DAP coated PBMA 8% SNC (Bar scale: 20 µm)

The C, N and O elements show a more homogeneous distribution on the cross-section of DAP coated with the copolymer (Fig. 7A). However, the detection of nutrients such as P and N in the coating layers, which are present in small quantities (Fig 7B), indicates that this nutrient penetrates into the coating layer. In fact, during the dip-coating process, the DAP fertilizer was

successively immersed in the aqueous emulsion solution of both PBMA homopolymer and P(BMA-*co*-PFA) copolymer, leading to the diffusion of N and P nutrients in the coating as the DAP fertilizer granules are soluble in water.

3-2-2 Phosphorous and Nitrogen release behaviors of coated and uncoated DAP Fertilizers

The nutrient release rates of uncoated and coated DAP granules of fertilizer in distilled water and room temperature are described according to the procedures reported by Li et al. [55] and Pereira et al. [56]. Figure 8 exhibits the percentages of P and N released in water *versus* time of the coated DAP from PBMA and P(BMA-*co*-PFA) polymers, and the uncoated DAP at pH 7 and room temperature.

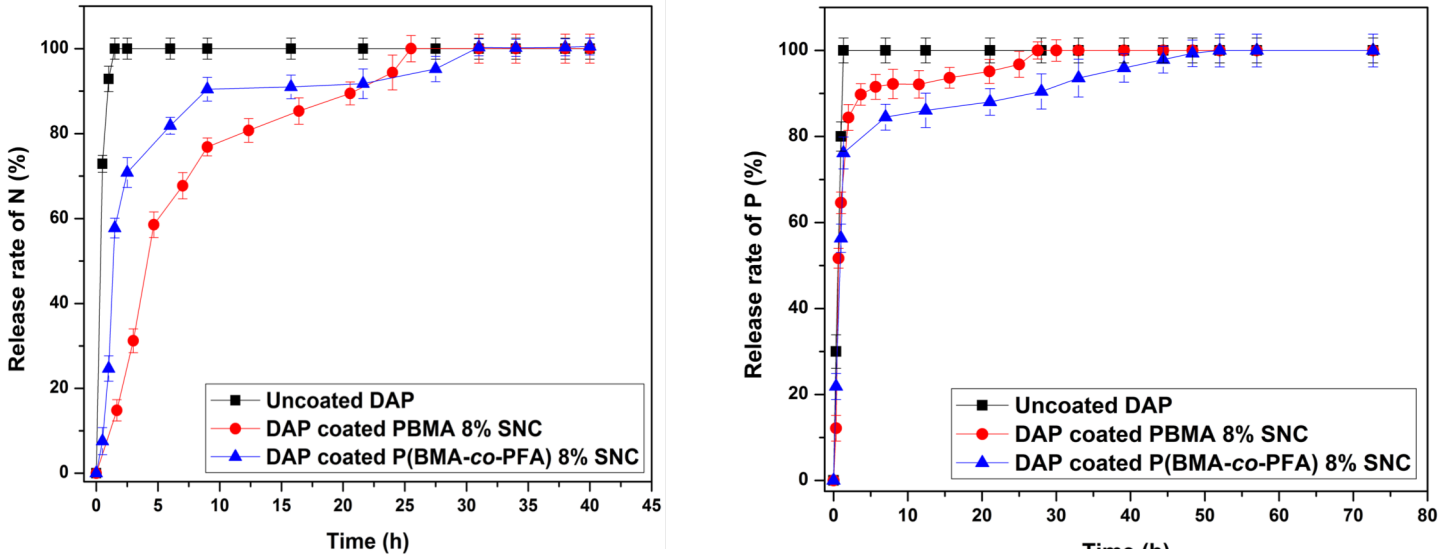

Figure 8. Kinetics of N and P releases in the case of uncoated DAP and coated DAP with P(BMA-*co*-PFA) 8 wt. % SNC and DAP coated with PBMA 8 wt. % SNC in water at pH 7 at room temperature.

Figure 8 shows that the release behavior occurred in two stages. At the beginning of the release period, the N release rate of coated DAP with both PBMA and P(BMA-*co*-FPA) (co)polymers increases rapidly from 0 to 5-10 hours (1st stage: fast release) and then gradually increased from 5-10 hours to 25-30 hours (2nd stage: slow release). A similar profile is observed for P release from both coating materials. Finally, the complete releases of N and P, from PBMA and P(BMA-*co*-FPA) coatings, corresponding to a saturation plateau are reached after 27-32 hours and 28-50 hours, respectively.

Figure 8 also displays that the nutrient solubilisation rate in water is much slower in the case of

encapsulated fertilizers than for uncoated DAP. The untreated DAP is totally solubilized after 2 hours, while the P release profile of the coated granules reached the equilibrium stage approximatively after 28 and 50 hours when the DAP is coated with PBMA and P(BMA-*co*-FPA), respectively. Indeed, the time to reach the maximum concentration of N release is 13.5 and 16.0 times lower than the corresponding uncoated DAP when the DAP granules are covered with PBMA and P(BMA-*co*-FPA), respectively, indicating significant slower P release properties. Therefore, these coatings have a great potential in increasing the fertilizer use efficiency significantly. [7, 18, 20] The P(BMA-*co*-FPA) coating exhibited a much delaying release of nutrients than that of PBMA. In fact, in 24 hours, the former just delivered 85% of the total nutrient whereas the latter one nearly released completely, providing that the chemical structure of the coating is one of the key parameters affecting the release behavior of P nutrient from the coating. In fact, considering the above contact angle results, the enhancement of hydrophobicity of fertilizer coated with P(BMA-*co*-PFA) was expected to contribute to the slow release of nutrients due to the presence of the fluorinated comonomer with water repellent properties attributed to $-C_6F_{13}$ side groups even at low incorporation (6.5 mol%) of FPA commoner. [24] In addition, the thickness of the coating is also an important parameter that can significantly govern the nutrient release. In fact, an increasing coating thickness resulted in low nutrients release as the coating exhibited a long resistance path which hinders the nutrient diffusion. [57] In our case, the thickness of P(BMA-*co*-PFA) (39 µm) is slightly higher than that of PBMA (34 µm). Hence, it can be concluded the reason for which the fluorinated copolymer coating produced a longer duration of nutrients release.

3-2-3 Mathematical Modeling of Release Kinetics

To confirm the above interpretations on the behaviour of nutrient release in water and to describe the release kinetics and the transport mechanism of nutrient through the polymer coatings, the data curves (Figure 8) were fitted following the semi-empirical Ritger-Peppas model (Eq.1). [38] More details about this model and the corresponding mechanisms based on the diffusional exponent (n) characterizing the release mechanism are supplied in the Electronic Supporting Information (ESI). To obtain the n and k (release factors) values, graphs of $Log(M_t/M_\infty)$ *versus* Log(t) were plotted (According to Eq. 1, Figure S3) for each release nutrients of DAP coated with PBMA and P(BMA-*co*-PFA). The n and k coefficients were obtained from the angular coefficient and linear coefficient of the straight line, respectively. Table 4 summarizes the resulting data of N and P nutrient releases from both polymers

corresponding to the first and second release stages. The correlation coefficient (R^2) was higher than 0.9 in all cases.

Based on the results presented in Table 3, all calculated n-values of the first stage are greater than 1, except for DAP coated with P(BMA-*co*-PFA) for P release which has a n-value close to 1 (n = 0.90). These results indicate that the release is highly retained by the polymer barrier, that the diffusion is carried out gradually allowing to the diffusion (accelerating the process) by opening pores or degrading the structure of polymer coating (erosion of polymer). [39,58] A n-value close to 1, corresponding to the release test of P for DAP coated with P(BMA-*co*-PFA), indicates that this sample probably has significant uncoated parts where the dissolution takes place without any barrier. [58] It is also reported that solely the molecular relaxation is responsible for nutrient transport in this case. [39]

Table 4. Kinetic parameters of N and P releases calculated according to the Ritger-Peppas model from DAP coated with P(BMA-*co*-PFA) 8 wt. % SNC and PBMA 8 wt. % SNC.

			Release exponent (n) [a]	Release factor k (h^{-1}) [a]	Correlation coefficient (R^2)	Diffusion Coefficient D x 10^{10} (cm^2/s) [b]
1st stage (fast release)						
DAP coated	P(BMA-*co*-FPA)	P	0.90	0.79	0.99	2.66
		N	1.83	0.56	0.99	0.51
	PBMA	P	1.09	0.75	0.90	2.58
		N	1.34	0.31	0.99	0.14
2nd stage (slow release)						
DAP coated	P(BMA-*co*-FPA)	P	0.05	0.89	0.90	1.40
		N	0.13	0.82	0.93	1.08
	PBMA	P	0.04	0.92	0.91	1.36
		N	0.22	0.71	0.97	0.45

[a] Calculated from Eq 1
[b] Calculated from Eq 2

However, for the second stage, all n values are lower than 0.5. These results are in agreement with a quasi-Fickian diffusion mechanism which characterized a partial diffusion. Thus, nutrients diffuse partially through a swollen matrix as a result of structural rearrangements in the polymer support. [59]

Indeed, the diffusion coefficient values (D) for P and N releases from both polymer coatings, obtained from Eq.2, are given in Table 4. By analysing and comparing k and D values, Table 2 reveals that for the fast release of P (first stage), $k_{(P(BMA\text{-}co\text{-}FPA)/P)}$ (0.79 h^{-1}) ≈ $k_{(PBMA/P)}$ (0.75 h^{-1}) and $D_{(P(BMA\text{-}co\text{-}FPA)/P)}$ (2.66 10^{-10} cm^2/s) ≈ $D_{(PBMA/P)}$ (2.58 10^{-10} cm^2/s), while $k_{(P(BMA\text{-}co\text{-}FPA)/N)}$ (0.56 h^{-1}) > $k_{(PBMA/N)}$ (0.31 h^{-1}) and $D_{(P(BMA\text{-}co\text{-}FPA)/N)}$ (0.51 10^{-10} cm^2/s)> $D_{(PBMA/N)}$ (0.14 10^{-10} cm^2/s) for N release. For the slow release (second stage), it is noted that $k_{(P(BMA\text{-}co\text{-}FPA)/P)}$ (0.89 h^{-1})≈ $k_{(PBMA/P)}$ (0.92 h^{-1}) and $D_{(P(BMA\text{-}co\text{-}FPA)/P)}$ (1.40 10^{-10} cm^2/s) ≈ $D_{(PBMA/P)}$ (1.36 10^{-10} cm^2/s) for the case of P, and $k_{(P(BMA\text{-}co\text{-}FPA)/N)}$ (0.82 h^{-1}) > $k_{(PBMA/N)}$ (0.71 h^{-1}) and $D_{(P(BMA\text{-}co\text{-}FPA)/N)}$ (1.08 10^{-10} cm^2/s) > $D_{(PBMA/N)}$ (0.45 10^{-10} cm^2/s) for the case of N.

Based on the above experimental comparison, it is clearly noted that the kinetics parameters (k and D) for the P release (first stage and second stage) are partially equal for both coating (co)polymers (Figure 8). However, in the case of N release, these parameters are small for PBMA compared to P(BMA-*co*-PFA) for the first and second stages as observed in the release curves (Figure 8).

Conclusion

Stable coagulum free latex dispersions based on butyl methacrylate (BMA) and 2-(perfluorohexyl)ethyl acrylate (PFA) were synthesized via emulsion (co)polymerization using SNC as a sole stabilizer in replacement of synthetic surfactant. The size of the polymer particles was in the range of 200-300 nm, depending on the SNC content and the dispersion was stable for several months. The low percentage of incorporated PFA (6.5 %) in P(BMA-*co*-PFA), increased the hydrophobic character of the film, as evidenced by the increase of the water contact angle of the corresponding films compared to that of the PBMA homopolymer. However, the evolution in the contact angle was dependent on the amount of added SNC, with the highest value was observed at 10% SNC. A decrease of Tg by about 10 °C in comparison with that of PBMA homopolymer was also observed for the copolymer, facilitating the film-formation of the latex at a temperature 15-25 °C. The morphology of the surface and cross-section of coated DAP fertilizer with both (co)polymers was studied by SEM, EDX and mapping to calculate the thickness of the coating membrane and also to evaluate the adhesion between the DAP and the coating films. The profile release of N and P from DAP covered coating films was performed using a UV-vis spectrophotometer. This encapsulation expands the P release to 28 and 50 hours instead of only 2 h for uncoated DAP. Indeed, the time to reach maximum concentration of N release was 13.5 and 16.0 times than the corresponding

uncoated DAP when the DAP is covered with PBMA and P(BMA-*co*-FPA), respectively. Compared to PBMA, the kinetic study also shows that P(BMA-*co*-PFA) copolymer exhibits better slow release properties even at low percentage of PFA (6.5 mol%) due to C_6F_{13} side group inducing to the copolymer better hydrophobic character and lower T_g with improved film-forming properties. Therefore, the copolymer exhibited promising application as waterborne copolymer for enhancing the efficiency of fertilizer and minimize their impact on the environment.

The porosity of the coating polymers plays an important role in slow and controlled release of nutrients from the coated fertilizers. Innovative approaches are needed to improve the soil water balance for the crops in the arid and semi-arid regions. In fact, the preparation of superabsorbent polyacrylate hydrogels with improved water-holding capacity, and water-retention properties using emulsion copolymerisation and crosslinking reactions led to semi-interpenetrating polymer networks (Semi-IPN). The preparation of Semi-IPN based on (co)polymers of BMA and PFA by emulsion (co)polymerization using starch nanocrystals (SNC) as a pickering stabilizer and in the presence of N,N'-methylenebisacrylate (MBA) as a cross-linking agent to obtain networks with water-retention capacity and slow release nutrients performances is under investigation.

Acknowledgments

The authors thank the support through the R&D Initiative -Call project APPHOS-sponsored by Office Chérifien de Phosphates OCP, OCP Foundation, R&D OCP, Mohammed VI Polytechnic University, National Centre of Scientific and Technical Research CNRST, Ministry of Higher Education, Scientific Research and Professional Training of Morocco MESRSFC (project ID: VAL-RAI-01/2017).

Notes: The authors declare no competing financial interest.

Author Contributions:

A. Sofyane : Investigation, Formal analysis, Writing - original draft.
E. Ben Ayed : Investigation, Formal analysis, Writing - original draft.
M. Elrebii : Analysis and interpretation of the data.
M. Lahcini : Investigation, Review & editing.
H. Kaddami: Formal analysis and interpretation of the data, Review & editing.
H. Khouloud: Resources, Validation, Approval of the final version.
B. Ameduri : Analysis and interpretation of the data, Review & editing.
S. Boufi : Conceptualization, supervision, Review & editing.
M. Raihane: Conception and design, supervision, Review & editing and Resources.

The manuscript was written through contributions of all authors. All authors have given approval to the final version of the manuscript.

References

[1] N. Alexandratos, J. Bruinsma, World Agriculture Towards 2030 / 2050 : The 2012 Revision, Food and Agricultural Organization (FAO), Rome, (2012), available online at http://www.fao.org/fileadmin/templates/esa/Global_persepctives/world_ag_2030_50_2012_rev.pdf, Accessed on 15 December 2020.

[2] W. M. Stewart, T. L. Roberts, Food Security and the Role of Fertilizer in Supporting it, Procedia Engineering. 46 (2012) 76–82. https://doi:10.1016/j.proeng.2012.09.448.

[3] M. C. DeRosa, C. Monreal, M. Schnitzer, R. Walsh, Y. Sultan, Nanotechnology in fertilizers, Nat. Nanotechnol. 5 (2010) 91. https:// doi: 10.1038/nnano.2010.2.

[4] D. Tilman, J. Fargione, B. Wolff, C. D'Antonio, A. Dobson, R. Howarth, D. Schindler, W. H. Schlesinger, D. Simberloff, D. Swackhamer, Forecasting Agriculturally Driven Global Environmental Change, Science. 292 (2001) 281-284. http://doi: 10.1126/science.1057544.

[5] M. Guo, M. Liu, R. Liang, A. Niu, Granular urea-formaldehyde slow-release fertilizer with superabsorbent and moisture preservation, J App Polym Sci. 99 (2006) 3230. http://doi:10.1002/app.22892.

[6] Y. Shang, Md. K. Hasan, G. J. Ahammed, M. Li, H. Yin, J. Zhou, Applications of nanotechnology in plant growth and crop protection, Molecules. 24 (2019) 2558. http:// 10.3390/molecules24142558.

[7] B. Azeem, K. KuShaari, Z. B. Man, A. Basit, T. H. Thanh, Review on materials & methods to produce controlled release coated urea fertilizer, J Controlled Release. 181 (2014) 11-21. https:// doi.org/10.1016/j.jconrel.2014.02.020.

[8] D. Qiaoa, H. Liu, L. Yu, X. Bao, G. P. Simon, E. Petinakisc, L. Chena, Preparation and characterization of slow-release fertilizer encapsulated by starch-based superabsorbent polymer, Carbohydrate Polymers. 147 (2016) 146–154. https://doi.org/10.1016/j.carbpol.2016.04.010.

[9] P. Wen, Z. Wu, Y. He, B. Ye, Y. Han, J. Wang, X. Guan, Microwave-assisted synthesis of a semi-IPN slow-release nitrogen fertilizer with Water Absorbency from Cotton Stalks, ACS Sustainable Chemistry & Engineering. 4 (2016) 6572-6579. http://doi.org/10.1021/acssuschemeng.6b01466.

[10] A. Shaviv, Advances in controlled-release fertilizers, Advances in Agronomy 71 (2001) 1-49. http://doi:10.1016/s0065-2113(01)71011-5.

[11] X. Yang, Y. Cao, R. Jiang, Effect of atomization on membrane structure and characteristics during manufacture of polymer coated controlled-release fertilizer, Journal of Chemical Industry and Engineering (China). 59 (2008) 778–784. http://en.cnki.com.cn/Article_en/CJFDTOTAL-HGSZ200803039.htm.

[12] S. Ahmad, S. M. Ashraf, U. Riaz, S. Zafar, Development of novel waterborne poly(1-naphthy lamine)/poly(vinylalcohol)-resorcinol formaldehyde-cured corrosion resistant composite coatings, Progress in Organic Coatings. 62 (2008) 32–39. http://doi.org/10.1016/j.porgcoat.2007.09.014.

[13] A. Rashidzadeh, A. Olad, Slow-released NPK fertilizer encapsulated by NaAlg-g-poly(AA-co AAm)/MMT superabsorbent nanocomposite, Carbohydrate Polymers. 114 (2014) 269-278. https://doi.org/10.1016/j.carbpol.2014.08.010.

[14] Y. Shen, C. Zhao, J. Zhou, C. Du, Application of waterborne acrylic emulsions in coated controlled release fertilizer using reacted layer technology, Chinese Journal of Chemical Engineering. 23 (2015) 309–314. https://doi.org/10.1016/j.cjche.2014.09.034.

[15] X. An, J. Yu, J. Yu, A. Tahmasebi, Z. Wu, X. Liu, B. Yu. Incorporation of biochar into semi-interpenetrating polymer networks through graft co-polymerization for the synthesis of new slow-release fertilizers, Journal of Clener Production. 272 (2020) 122731. https://doi.org/10.1016/j.jclepro.2020.122731.

[16] Z. Zhou, Y. Shen, C. Du, J. Zhou, Y. Qin, Y. Wu, Economic and soil environmental benefits of using controlled-release bulk blending urea in the north china plain, Land Degradation and Development. 28 (2017) 2370–2379. https://doi.org/10.1002/ldr.2767.

[17] Chemtex Speciality Limited, 2011, Haute Street Corporate Park, 86A Topsia Road (S), Kolkata 700046, India. https://www.hydrogelagriculture.com.

[18] S. Ghazali, S. Jamari, N. Noordin, K. M. Tan. Properties of Controlled-Release-Water-Retention Fertilizer Coated with Carbonaceous-g-Poly(acrylic acid-co-acrylamide)Superabsorbent Polymer, International Journal of Chemical Engineering and Applications. 8 (2017) 141-147. http://doi.org/10.18178/ijcea.2017.8.2.646.

[19] S. Li, G. Chen, Agricultural waste-derived superabsorbent hydrogels : Preparation, performance, and socioeconomic impacts, Journal of Cleaner Production. 251 (2020) 119669. https://doi.org/10.1016/j.jclepro.2019.119669.

[20] J. Song, H. Zhao, G. Zhao, Y.Xiang, Y. Liu, Novel Semi-IPN Nanocomposites with Functions of both Nutrient Slow-Release and Water Retention. 1. Microscopic Structure, Water Absorbency, and Degradation Performance, Journal of Agricultural and Food Chemistry. 67 (2019) 7587.

https://doi.org/10.1021/acs.jafc.9b00888.
[21] b. Wilske, M. Bai, B. Lindenstruth, M. Bach, Z. Rezaie, H. G. Frede, L. Breuer, Biodegradability of a polyacrylate superabsorbent in agricultural soil. Environmental Science and Pollution Research. 21 (2013) 9453–9460. https://doi.org/10.1007/s11356-013-2103-1.
[22] A. Olad, M. Pourkhiyabi, H. Gharekhani, F. Doustdar, Semi-IPN superabsorbent nanocomposite based on sodium alginate and montmorillonite: Reaction parameters and swelling characteristics, Carbohydrate Polymers. 190 (2018) 295-306. https://doi.org/10.1016/j.carbpol.2018.02.088.
[23] H. Ferfera-Harrar, N. Aiouaz, N. Dairi, A. S. Hadj-Hamou. Preparation of Chitosan-g-Poly(acrylamide) /Montmorillonite Superabsorbent Polymer Composites: Studies on Swelling, Thermal, and Antibacterial Properties, Journal of Applied Polymer Science 31 (2014) 39747. https://doi.org/10.1002/app.39747.
[24] W. Yao, Y. LI, X. Huang. Fluorinated poly(meth)acrylate: Synthesis and properties, Polymer 55 (2014) 6197-6211. https://doi.org/10.1016/j.polymer.2014.09.036.
[25] R. Ishige, T. Shinohara, K. L. White, A. Meskini, M. Raihane, A. Takahara, B. Ameduri, Unique Difference in Transition Temperature of Two Similar Fluorinated Side Chain Polymers Forming Hexatic Smectic Phase: Poly{2-(perfluorooctyl)ethyl acrylate} and Poly{2-(perfluorooctyl)ethyl vinyl ether}, Macromolecules 47 (2014) 3860−3870. https://doi.org/10.1021/ma500503z.
[26] F. Signori, M. Lazzari, V. Castelvetro, O. Chiantore. Copolymers of Isopropenyl Alkyl Ethers with Fluorinated Acrylates and Fluoroacrylates: Influence of Fluorine on Their Thermal, Photochemical, and Hydrolytic Stability, Macromolecules 39 (2006) 1749-1758. https://doi.org/10.1021/ma051672i.
[27] B. P. Koiry, H. A. Klok, N. K. Singha. Copolymerization of 2,2,3,3,4,4,4-heptafluorobutyl acrylate with butyl acrylate via RAFT polymerization, Journal of Fluorine Chemistry 165 (2014) 109-115. https://doi.org/10.1016/j.jfluchem.2014.06.016.
[28] E. Alyamac, M. D. Soucek. Acrylate-based fluorinated copolymers for high-solids coatings, Progress in Organic Coatings. 71 (2011) 213-22. https://doi.org/10.1016/j.porgcoat.2011.02.015.
[29] S. Chen, Y. Han, M. Yang, X. Zhu, C. Liu, H. Liu, H. Zou . Hydrophobically modified water-based polymer for slow-release urea formulation, Progress in Organic Coatings. 149 (2020) 105964. https://doi.org/10.1016/j.porgcoat.2020.105964.
[30] W. Yuan, Y. Shen, F. Ma, C. Du. Application of Graphene-Oxide-Modified Polyacrylate Polymer for Controlled-Release Coated Urea, Coatings. 8 (2018) 64. https://doi.org/ doi:10.3390/coatings8020064.
[31] M. Errezma, A. Mabrouk, A. Magnin, A. Dufresne, S. Boufi. Surfactant-free emulsion Pickering polymerization stabilized by aldehyde functionalized cellulose nanocrystals, Carbohydrate Polymer. 202 (2018) 621–630. https://doi.org/10.1016/j.carbpol.2018.09.018.
[32] S. Cummings, E. Trevino, Y. Zhang, M. Cunningham, M.A. Dubé, Incorporation of modified regenerated starch nanoparticles in emulsion polymer latexes, Starch/Starke. 71 (2018) 1800192. https://doi.org/10.1002/star.201800192.
[33] W. Thielemans, M.N. Belgacem, A. Dufresne, Starch nanocrystals with large chain surface modifications, Langmuir. 22 (2006) 4804-4810. https://doi.org/10.1021/la053394m.
[34] H. Angellier, L. Choisnard, S. Molina-Boisseau, P. Ozil, A. Dufresne, Optimization of the preparation of aqueous suspensions of waxy maize starch nanocrystals using a response surface methodology, Biomacromolecules. 5 (2004) 1545–1551. https://doi.org/10.1021/bm049914u.
[35] T. Li, B. Gao, Z. Tong, Y. Yang, Y. Li, Chitosan and graphene oxide nanocomposites as coatings for controlled-release fertilizer, Water Air Soil Pollution. 230 (2019) 146. https://doi.org/ 10.1007/s11270-019-4173-2.
[36] J. Li, M. Wang, D. She, Y. Zhao, Structural functionalization of industrial softwood kraft lignin for simple dip-coating of urea as highly efficient nitrogen fertilizer, Industrial Crops and Product. 109 (2017) 255–265. https://doi.org/10.1016/j.indcrop.2017.08.011.
[37] A. Sofyane, E. Ablouh, M. Lahcini, A. Elmeziane, M. Khouloud, H. Kaddami, M. Raihane. Slow-Release Fertilizers Based on Starch acetate/ Glycerol/ Polyvinyl Alcohol biocomposites for Sustained Nutrient Release. Materials Today : Proceedings. (2020). https://doi.org/10.1016/j.matpr.2020.05.319.
[38] P. L. Ritger, N. A. Peppas, A simple equation for description of solute release, Journal of Controlled Release. 5 (1987) 23–36. https://doi.org/10.1016/0168-3659(87)90034-4
[39] R. Bortoletto-Santos, C. Ribeiro, W. L. Polito, W.Controlled release of nitrogen-source fertilizers by natural-oil-based poly(urethane) coatings: The kinetic aspects of urea release, Journal of Applied Polymer Science. 133 (2016) 1–8. https://doi.org/10.1002/app.43790.
[40] J. M. Geurts, *P.E.* Jacobs, *J. G.* Muijs, S. J. J. G. Van Es, A. L. German, Journal of Applied Polymer Science. 61 (1996) 9-19.
[41] S. Beuermann, M. Buback, T. P. Davis, R. G. Gilbert, R. A. Hutchinson, A. Kajiwara, B. Klumperman, G. T. Russell, Critically evaluated rate coefficients for free-radical polymerization, 3. Propagation rate coefficients for alkyl methacrylates, Macromolecular Chemistry and Physics. 201(2000) 1355. https://doi.org/10.1002/1521-3935(20000801)201:12<1355::AID-MACP1355>3.0.CO;2-Q.

[42] V. Castelvetro, C. De Vita, G. Giannini, S. Giaiacopi, Role of anionic and nonionic surfactants on the control of particle size and latex colloidal stability in the seeded emulsion polymerization of butyl methacrylate, Journal of Applied Polymer Science. 102 (2006) 3083–3094. https://doi.org/10.1002/app.23717
[43] A. T.; Price, C.P. Charles. Relative reactivities in vinyl copolymerization, Journal of Polymer Science. 2 (1947) 101–106. https://doi.org/10.1002/pol.1947.120020112.
[44] E. Ben Ayed, A. Magnin, J. L. Putaux, S. Boufi, Vinyltriethoxysilane-functionalized starch nanocrystals as Pickering stabilizer in emulsion polymerization of acrylic monomers. Application in nanocomposites and pressure-sensitive adhesives, Journal of Colloid and Interface Science. 587 (2020) 533-546. https://doi.org/10.1016/j.jcis.2020.05.011.
[45] Y. Chevalier, M. A. Bolzinger, Emulsions stabilized with solid nanoparticles: Pickering emulsions, Colloids and Surfaces A: Physicochemical and Engineering Aspects. 439 (2013) 23–34. https://doi.org/10.1016/j.colsurfa.2013.02.054
[46] N. Kohut-Svelko, R. Pirri, J. M. Asua, J. R. Leiza, Redox initiator systems for emulsion polymerization of acrylates, Journal of Polymer Science Part A: Polymer Chemistry. 47 (2009) 2917–2927. https://doi.org/10.1002/pola.23362.
[47] S.B. Haaj, A. Magnin, S. Boufi, Starch nanoparticles produced via ultrasonication as a sustainable stabilizer in Pickering emulsion polymerization, RSC Advances. 4 (2014) 42638–42646. https://doi.org/ 10.1039/C4RA06194B.
[48] E. Barbu, R. A. Pullin, P. Graham, P. Eaton, R. J. Ewen, J. D. Smart, T. G. Nevell, J. Tsibouklis,. Poly(di-1H,1H,2H,2H-perfluoroalkylitaconate) films: surface organisation phenomena, surface energy determinations and force of adhesion measurements, Polymer. 43 (2002) 1727-1734. https://doi.org/10.1016/S0032-3861(01)00777-7.
[49] L. Ren, Y. Zhang, Q. Wang, J. Zhou, J. Tong, D. Chen, X. Su, Convenient Method for Enhancing Hydrophobicity and Dispersibility of Starch Nanocrystals by Crosslinking Modification with Citric Acid, International Journal of Food Engineering. 14 (2018) 1556-3758. https://doi.org/10.1515/ijfe-2017-0238.
[50] P. K. Dhal, G. N. Babu, J. C. W. Chien, Resist polymers: part VII thermolysis of fluoroalkyl methacrylates, Polymer Degradation and Stability. 16 (1986) 135-145. https://doi.org/10.1016/0141-3910(86)90058-3.
[51] V. Castelvetro, M. Raihane, S. Bianchi, S. Atlas, I. Bonaduce. Thermal degradation behaviour of a nearly alternating copolymer of vinylidene cyanide with 2,2,2-trifluoroethyl methacrylate, Polymer Degradation and Stability. 96 (2011) 204-211. https://doi.org/10.1016/j.polymdegradstab.2010.11.016.
[52] A. Dubey, D. R. Mailapalli, Zeolite coated urea fertilizer using different binders : Fabrication, material properties and nitrogen release studies, Environmental Technology & Innovation. 16 (2019) 100452. https://doi.org/10.1016/j.eti.2019.100452.
[53] S. Fertahi, I. Bertrand, M. Amjoud, A. Oukarroum, M. Arji, A. Barakat, Properties of Coated Slow-Release Triple Superphosphate (TSP) Fertilizers Based on Lignin and Carrageenan Formulations, ACS Sustainable Chemistry & Engineering. 7 (2019) 10371-10382. https://doi.org/10.1021/acssuschemeng.9b00433.
[54] OCP (2019). https://www.ocpgroup.ma/sites/default/files/2016-10/OCP_VAr-VFr_def_22-04 15_C_9.pdf. Accessed on 17 December 2020.
[55] T. Li, S. Lü, Y. Ji, T. Qi, M. Liu, A biodegradable Fe-fertilizer with high mechanical property and sustainable release for potential agriculture and horticulture applications, New journal of chemistry. 42 (2018) 19129-19136. https://doi.org/10.1039/c8nj04381g.
[56] E. I. Pereira, F. B. Minussi, C. C. T. da Cruz, A. C. C. Bernard, C. Ribeiro, Urea − Montmorillonite-Extruded Nanocomposites: A Novel Slow- Release Material, Journal of Agricultural and Food Chemistry. 60 (2012) 5267-5272. https://doi.org/10.1021/jf3001229.
[57] N. N. R. Ahmad, W. J. N. Fernando, M. H. Uzir, Parametric evaluation using mechanistic model for release rate of phosphate ions from chitosan- coated phosphorus fertiliser pellets, Biosystems Engineering. 129 (2014) 78-86. http://dx.doi.org/10.1016/j.biosystemseng.2014.09.015.
[58] D. Cruz, R. Bortoletto-Santos, G. Guimarães, W. L. Polito, C. Ribeiro, Role of polymeric coating on the phosphate availability as fertilizer: insight from phosphate release in soil castor polyurethane coatings, Journal of Agricultural and Food Chemistry. 65 (2017) 5890–5895. https://doi.org/10.1021/acs.jafc.7b01686.
[59] B. Azeem, K. KuShaari, Z. Man , Effect of Coating Thickness on Release Characteristics of Controlled Release Urea Produced in Fluidized Bed Using Waterborne Starch Biopolymer as Coating Material, Procedia Engineering. 148 (2016) 282 – 289. https://doi.org/10.1016/j.proeng.2016.06.615.